ELSEVIER

Chemical Engineering Journal 74 (1999) 99–108

Chemical Engineering Journal

Molecular modeling of fluid separations using membranes: effect of molecular forces on mass transfer rates

S. Murad*, J. Lin

Department of Chemical Engineering, University of Illinois at Chicago, Chicago, IL 60607, USA

Received 20 August 1998; received in revised form 5 January 1999; accepted 6 January 1999

Abstract

We report computer simulations of semi-permeable membranes using the method of molecular dynamics, to study solutions undergoing osmosis and reverse osmosis. These studies have been carried out at steady state, by periodically recycling solvent molecules that permeate the semi-permeable membrane. The method has been used to investigate the effect of a range of molecular forces, state conditions, and membrane morphology on the mass transfer rate of solvents across the membrane. These results could be used to test the accuracy of continuum, micro-continuum and statistical mechanical theories for transport across membranes, apart from being of intrinsic fundamental interest. © 1999 Elsevier Science S.A. All rights reserved.

Keywords: Mass transfer rates; Molecular dynamics; Semi-permeable membranes

1. Introduction

Osmosis and reverse osmosis are important processes that involve the separation of gaseous and liquid mixtures using semi-permeable membranes. In this paper we report computer simulation studies using a novel technique developed by us to model semi-permeable membranes realistically, based on an extension of the NVT molecular dynamics method [1]. The most important feature of our atomistic model is that it permits the permeability as well as the geometry of the membrane to be controlled directly, via its molecular parameters [2]. In addition the atoms or molecules that constitute the semi-permeable membrane are also allowed to vibrate or "wobble", as has been found to be essential for realistic simulations of zeolites [3]. In this paper we report an adaptation of this technique to allow processes under steady state conditions to be investigated. The method could previously be only used to follow the time evolution of a system to its final equilibrium condition, from an initial non-equilibrium state [2].

We will demonstrate the usefulness of this new technique, by using it to study the effect of a range of molecular interactions, the membrane morphology, and state conditions on the mass transfer rate across the membrane. These results, apart from being of intrinsic fundamental interest by themselves, can also be used to test the accuracy of various micro-continuum theories for reverse osmosis as well [4–6].

2. Method

Our non-steady state simulation method for studying osmosis has been described in detail previously [7–10] so we will only summarize it here. The molecules that constitute the membrane are tethered to their equilibrium positions by a simple harmonic potential:

$$\Phi = \tfrac{1}{2}K\delta^2. \tag{1}$$

Here K is the spring constant, while δ is the scalar distance between the actual position of a tethered membrane molecule, and its equilibrium position. The structure of a typical membrane and the simulation system are shown in Fig. 1. Most simulations were based on a nominal system of 1024 particles in the basic cyclically repeated parallelepiped, initially in an FCC configuration, with $L_x=4L_y=4L_z$. L_x was made larger than L_y and L_z to increase the distance between the planes of the two semi-permeable membranes. All molecules with $x=L_x/4$ and $3L_x/4$ in the initial FCC configuration were designated as the membrane molecules, and tethered to their FCC sites using the tethering potential given by Eq. (1). We have also done a limited number of

---

*Corresponding author. Tel.: +1-312-996-5593; fax: +1-312-996-0808; e-mail: murad@uic.edu

1385-8947/99/$ – see front matter © 1999 Elsevier Science S.A. All rights reserved.
PII: S1385-8947(99)00051-0

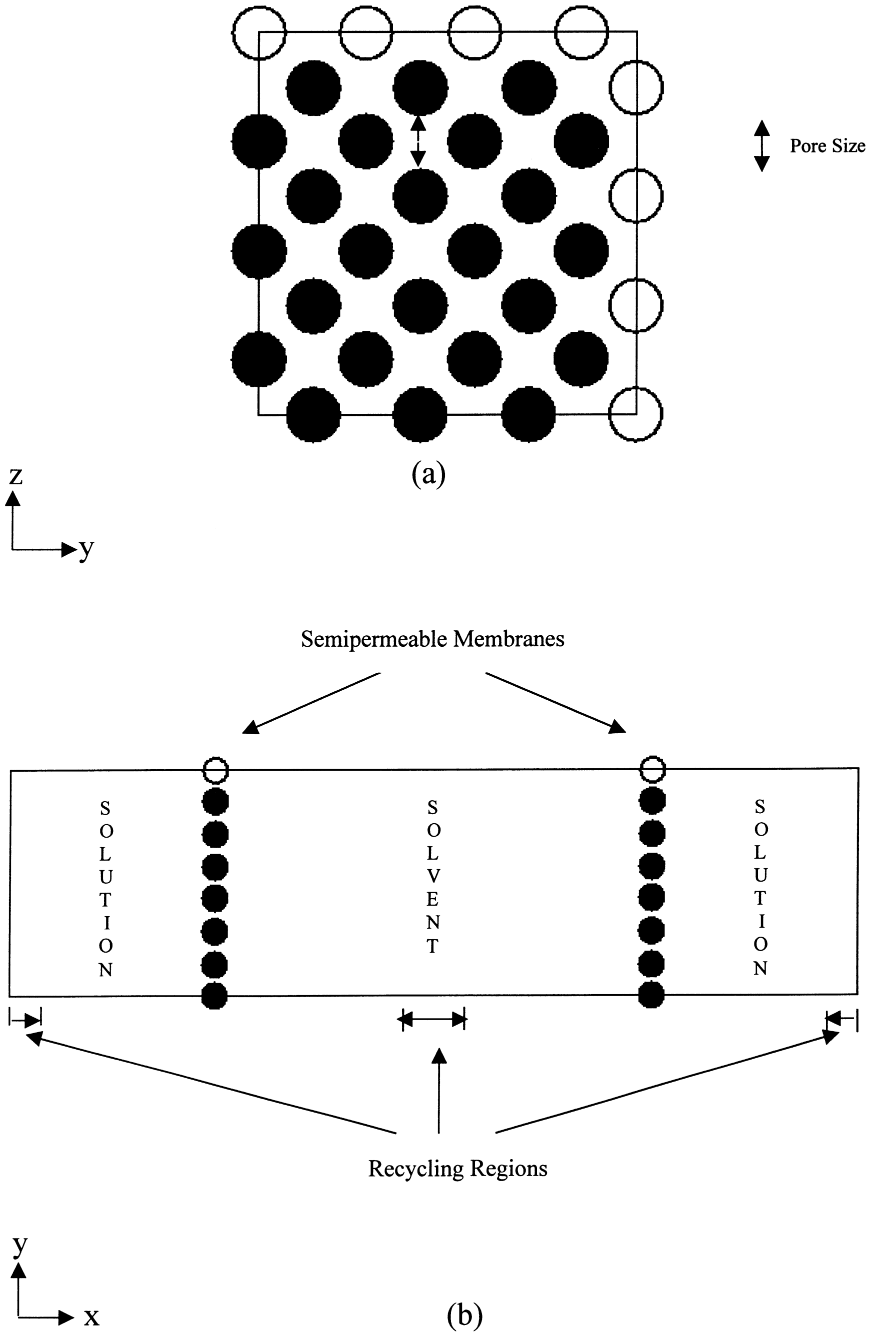

Fig. 1. A schematic diagram of: (a) the membrane structure (b) the simulation system. Periodic boundary conditions lead to a system infinite in the y and z directions with alternating solution and solvent compartments in the x direction separated by semi-permeable membranes.

simulations with membranes more than one molecular layer thick. This was done by adding a second mirror image layer of tethered molecules on the right of the existing membrane layers at $x=L_x/4$ and $3L_x/4$ at an appropriate distance from the first layer of molecules to model the desired membrane geometry. A layer of the original FCC molecules (near this layer) were also removed simultaneously to avoid overlapping molecules. This also conserved the total number of molecules in the simulation. We will refer to the one layer membrane as type I and the two layers as type II. A typical system with a type I membrane would have 64 molecules constituting the two membranes. 128 molecules would form the two type II membranes. The membrane molecules were tethered to their equilibrium positions as described above with a spring constant of 200 in reduced units. All results/parameters will be reported in reduced units based on the solute Lennard-Jones parameters. In the solution compartment (which consists of 480 or 448 molecules in total for type I and II membrane systems, respectively), N_B molecules are designated as solute molecules. The remaining

(480-N_B) particles, for example would then constitute the solvent molecules of the solution in the type I membrane case. N_B is fixed to correspond to the desired initial concentration of the solution being investigated, while the size of the simulation cell is fixed to correspond to the desired initial density of the solution. In the pure solvent compartment (see Fig. 1), since the size of the compartment is already fixed, we fix the initial number of solvent molecules N_S to correspond to the desired initial solvent density. In our studies reported here, the number density of the solvent compartment was always less than the solution compartment. Thus this step involved removing some molecules from the initial FCC configuration setup of the solvent compartment.

The method was adapted to study steady state processes based on a technique suggested recently [11], and similar in spirit to two recent methods suggested for steady state simulations [12,13], and involves recycling solvent molecules (that permeate the membrane) periodically. If done often enough this would result in a system approaching steady state. The molecules to be recycled were chosen randomly, one molecule at a time from a designated section of the solvent or solution compartment (as dictated by the direction in which solvent molecules permeate the membrane). This section was initially two units thick, and in the middle of the compartment (as far away from the membranes as possible as shown in Fig. 1(b)). They were then replaced (again one molecule at a time) at a random location in a similar section of the other compartment (solution or solvent as required), but only if it passed the usual Metropolis particle displacement requirement [14,15] widely used in Monte Carlo. This ensured that the recycling process, even though it was being carried out rather far away from the membrane (usually 10–20 solvent molecule layers away) did not produce any unusual disturbance in the system to affect the solvent permeation rate across the membrane. In some cases the width of these sections had to be increased to enable the particle recycling to be carried out successfully within a reasonable number of trials, but it was never in a region where it could affect the permeation of the solvent molecules across the membranes. This procedure is a simplification of the more rigorous schemes suggested in [12,13]. We were able to successfully use such a simplified scheme because we explicitly recycle the correct number of solvent molecules. This is done at a sufficient distance from the membranes, that the slight inconsistency introduced in our hybrid scheme does not affect the solvent permeation rate being calculated in our studies, while allowing us to use a much simpler algorithm. We carried out tests that showed that this did result in a system in steady state, or very close to it, since normal statistical fluctuations make it impossible to make an exact determination.

All molecular interactions were modeled using the Lennard-Jones intermolecular potential; this included the solute, solvent and the membrane molecules. As stated earlier, the membrane molecules were in addition also tethered. The parameters for these different interactions were always chosen to ensure that only the solvent molecules could permeate the semi-permeable membrane [7]. Several sets of interaction parameters (that satisfied this requirement) were investigated to measure their influence on the mass transfer rate of solvent molecules across the membrane. Cross-interactions were modeled using the Lorentz–Bertholet mixing rules, with the unlike interaction parameters set to unity. The simulations consisted of over 1 000 000 time steps of length 0.0025. The equations of motion were solved using a fifth order Gear predictor–corrector algorithm, with the usual periodic boundary conditions, and the nearest periodic image convention [1].

3. Results and discussion

The broad objective of this study was to investigate directly the effect of various molecular interactions on the permeation rate of solvents across the semi-permeable membrane, since they cannot be obtained unambiguously using theory [4]. We carried out an initial study with a "reference" intermolecular parameter set. This reference set in our studies consisted of (all parameters as stated earlier will be reported reduced by the solute parameters)

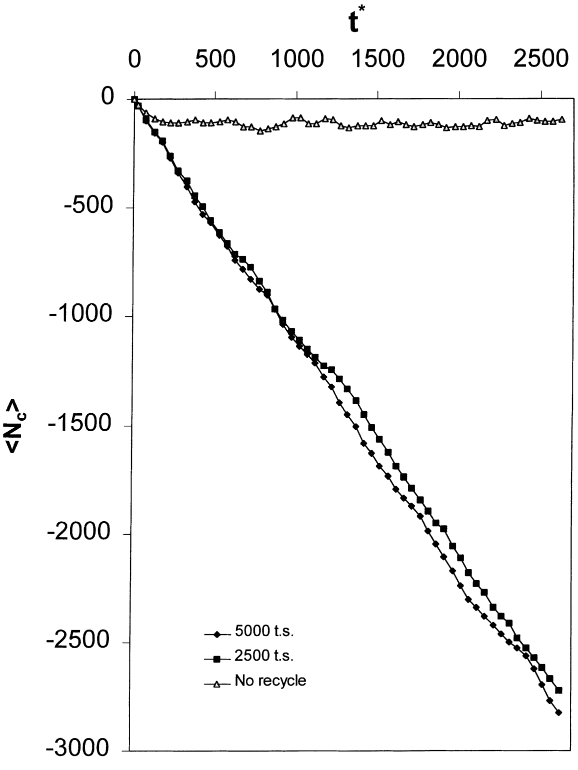

Fig. 2. Solvent permeation rates across the semi-permeable membrane with solvent recycling every 2500 or 5000 time steps. Also shown is the case where no recycling is carried out and the system is allowed to reach equilibrium. The points represent simulation results, while the lines in this and all subsequent figures are to guide the eye only.

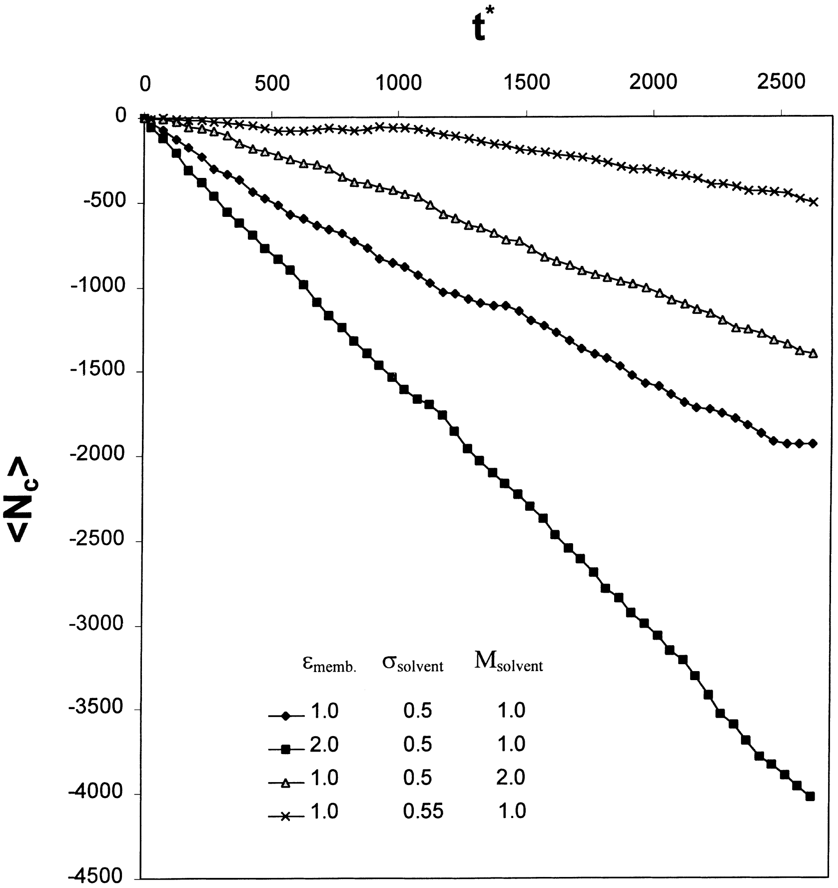

Fig. 3. Effect of changing $\varepsilon_{\mathrm{membrane}}$, $\sigma_{\mathrm{solvent}}$, and M_{solvent} on the solvent permeation rate across the semi-permeable membrane.

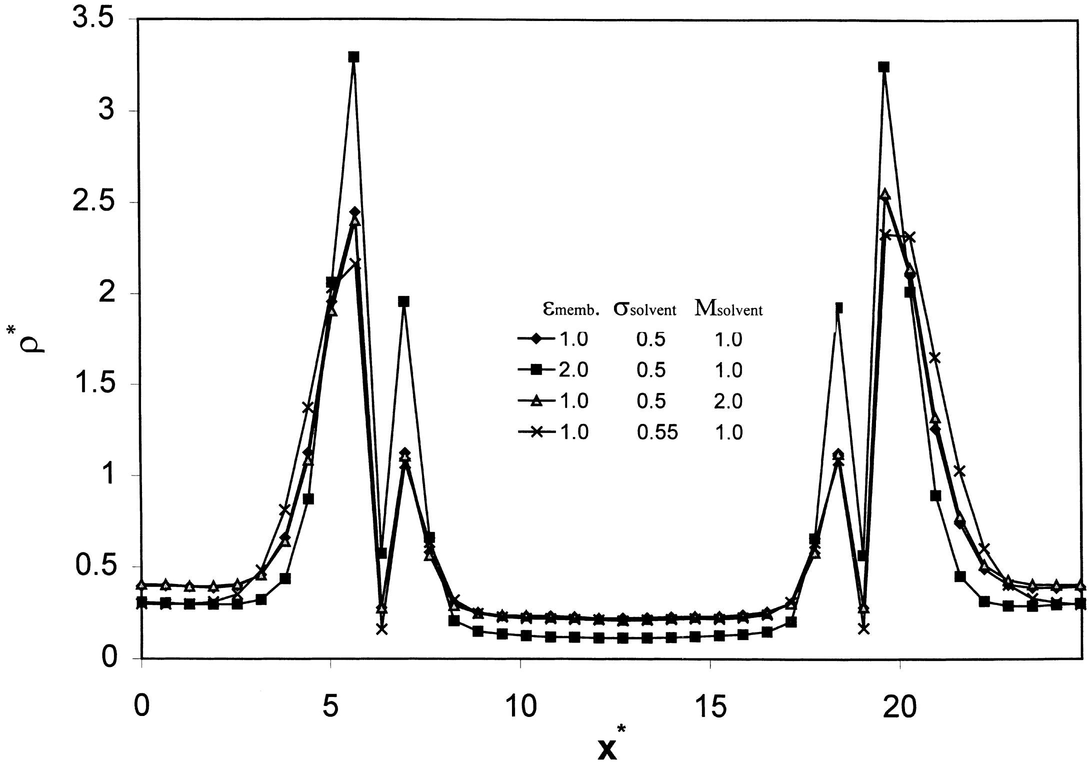

Fig. 4. Effect of changing $\varepsilon_{\mathrm{membrane}}$, $\sigma_{\mathrm{solvent}}$, and M_{solvent} on the density profiles of solvent molecules in the x-direction (perpendicular to the semi-permeable membranes).

solvent (ε, σ, M) values of (1, 0.5, 1). The pore size was fixed at 0.6 (as defined in Fig. 1), this corresponded to the LJ σ of the membrane molecules varying between 0.988 and 1.15 depending on the initial density of the system (see Section 2 for the membrane structure and Fig. 1). The LJ ε and the molecular weight of the molecules that constitute the membranes were both fixed at 1.0 for this reference set. We then investigated the effect of changing the LJ ε of the membrane molecules from 1 to 2, with everything else remaining unchanged. This would correspond to changing the membrane to one that has a stronger interaction with the solvent molecules – a more hydrophilic membrane for example, if the solvent were water [16]. We also looked at effect of increasing the molecular weight of the solvent molecules (this would be equivalent to having a solvent with a lower diffusion coefficient, without altering any other intermolecular interactions) from 1.0 to 2.0. Additionally we also investigated changes in the size of the solvent molecules, by increasing the σ of the solvent molecules from 0.5 to 0.55. This could be interpreted as reducing the pore to solvent diameter ratio, while keeping other variables constant. We would like to point out that molecular simulation studies are ideally suited to investigate such issues [17]. It is clearly not feasible to obtain this information experimentally directly, since it is virtually impossible to find species that differ from each other in only one molecular parameter, and it is not easy to obtain it using micro-continuum theories either [4].

The changes in the solvent permeation rates were also studied as a function of the most important osmotic driving forces, viz. density, temperature and composition. The solvent permeation rate, $\langle N_c \rangle$, is defined as

$$\langle N_c(t) \rangle = \left(\frac{1}{\delta t}\right) \int_{t-\delta t/2}^{t+\delta t/2} N_c(t')\, dt', \tag{2}$$

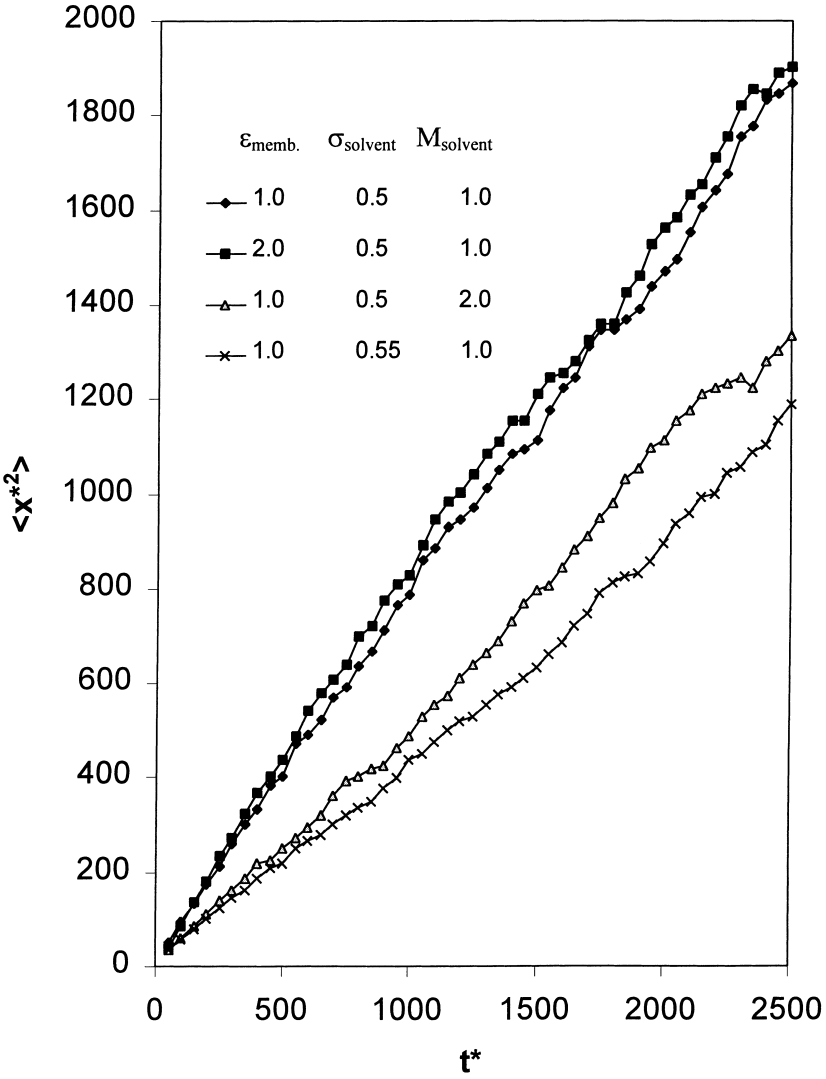

Fig. 5. Effect of changing $\varepsilon_{\text{membrane}}$, σ_{solvent}, and M_{solvent} on the mean squared displacement of the solvent molecules in the x-direction (perpendicular to the semi-permeable membranes).

where δt has been fixed at 20 000 time steps to average out any local fluctuations, and N_c is designated positive for flow from the solvent to the solution compartment. The recycling of the solvent molecules discussed above, was carried out every 5000 time steps, which on the average resulted in between 5 and 10 molecules being recycled in each such operation. Considering the size of our system (1024 molecules), this was found to be quite satisfactory. We also did a few studies in which recycling was done every 10 000 or 2500 time steps to examine the effect of the recycling rate on the solvent permeation rate. We found that all these recycle rates led to an almost constant mass flux across the membrane, within the expected fluctuations. The fluctuations were usually somewhat larger in the 10 000 steps recycle cases. A comparison of the solvent permeation rate for two recycling rates – every 5000 and 2500 time steps, is shown in Fig. 2 for a typical simulation. Also shown for comparison is the case when no recycling is carried out and the process is allowed to reach equilibrium. It is interesting to note that the initial mass transfer rate for the case with no recycling agrees well with the mass transfer rate for the two cases with solvent recycling. This serves to further validate the method.

Finally, we also looked at the effect of membrane thickness on the solvent permeation rate across the semi-permeable membrane. As described earlier this was accomplished by comparing two molecular layers thick membranes (with both layers of molecules identical) to membranes with only one layer of molecules. The second layer of membrane molecules was at a distance of $2^{1/6}\sigma_{\mathrm{membrane}}$ away from the first layer – this distance corresponds to the transition point between attractive and repulsive forces between the membrane molecules, and resulted in increasing the effective thickness of the membrane by a factor of more than 2. This

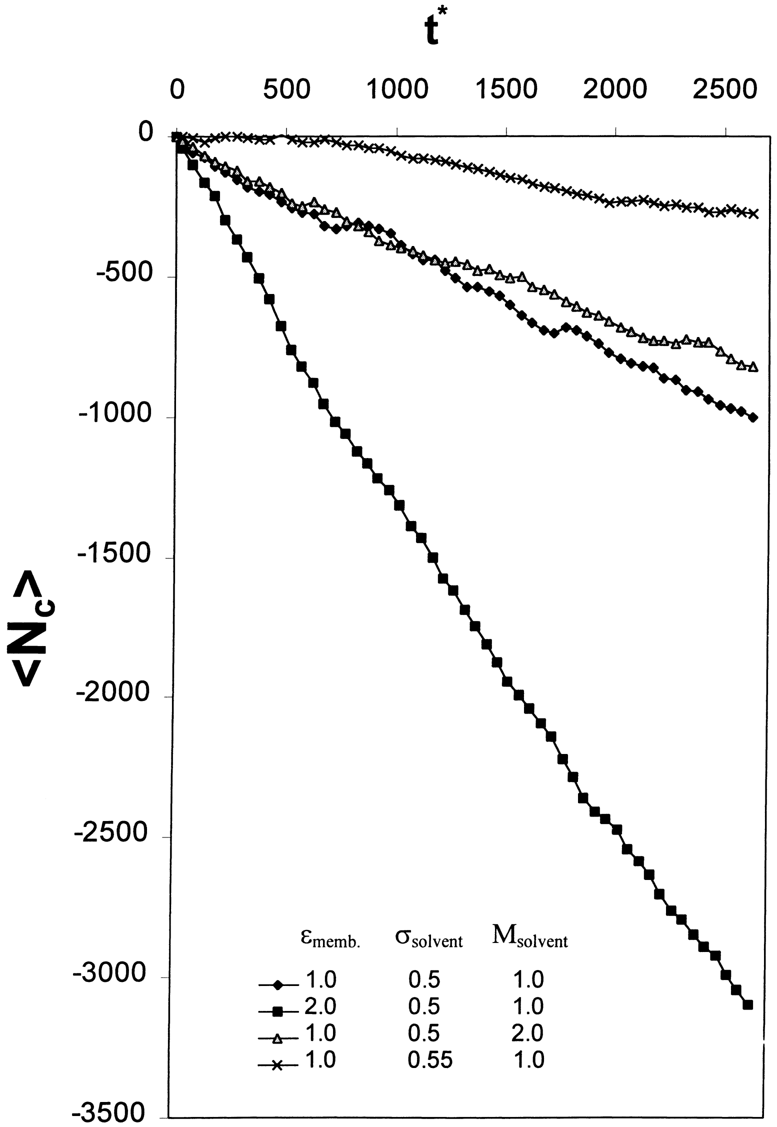

Fig. 6. Effect of changing $\varepsilon_{\mathrm{membrane}}$, $\sigma_{\mathrm{solvent}}$, and M_{solvent} on the solvent permeation rate across the semi-permeable membrane for a more concentrated solution (double the concentration of Fig. 3).

also ensured that there was no cross flow of solvent molecules between the two membrane layers.

The first set of simulations was carried out for type I membranes at a nominal reduced density, ρ^*(defined as $\rho\sigma^3$)=1.00, a reduced temperature $T^*(KT/\varepsilon) = 1.075$. This resulted in a system with $L_x^*(L_x/\sigma) = 25.4$, and L_y^* and $L_z^* = 6.35$. The solvent compartment initially had 180 solvent molecules, while the solution compartment had 460 solvent and 20 solute molecules. This resulted in a considerable pressure difference between the two compartments, as both compartments have equal volumes (see Fig. 1) and solvent mass flow from the solution to the solvent compartment. In these simulations, σ_{membrane} was fixed at 0.988, and $\varepsilon_{\text{solvent}}$ and M_{membrane} were both fixed at 1. We then investigated the effect of varying $\varepsilon_{\text{membrane}}$, σ_{solvent} and M_{solvent} on the rate of solvent permeation across the membrane. Fig. 3 shows the results for the number of solvent molecules permeating the membrane, $\langle N_c \rangle$, versus time, for these cases. It is seen that increasing $\varepsilon_{\text{membrane}}$ to 2.0 from 1.0 increases the permeation rate by almost a factor of 2, while increasing M_{solvent} to 2.0 from 1.0 decreases the permeation rate by about 30% and changing σ_{solvent} from 0.5 to 0.55 lowers the permeation rate by about 75%.

The results shown in Fig. 3 can be understood better if the density profiles and the mean squared displacements (msd) of the solvent molecules perpendicular to the membrane (in the x direction) are also examined. These have been shown in Figs. 4 and 5. It can be seen from Fig. 4 that when $\varepsilon_{\text{membrane}}$ is increased to 2.0 the peak of the solvent density profile near the membrane increases significantly (by about 35% on the solution side and 100% on the solvent side) due to increased solvent adsorption [18]. On the other hand Fig. 5 shows that the msd, and hence the diffusion coefficient is relatively unaffected by the change. The msd reported is averaged over all solvent particles; however, the displacement due to recycling is not included in the average. This shows that the increase in the permeation rate is primarily caused by the increased presence of the solvent

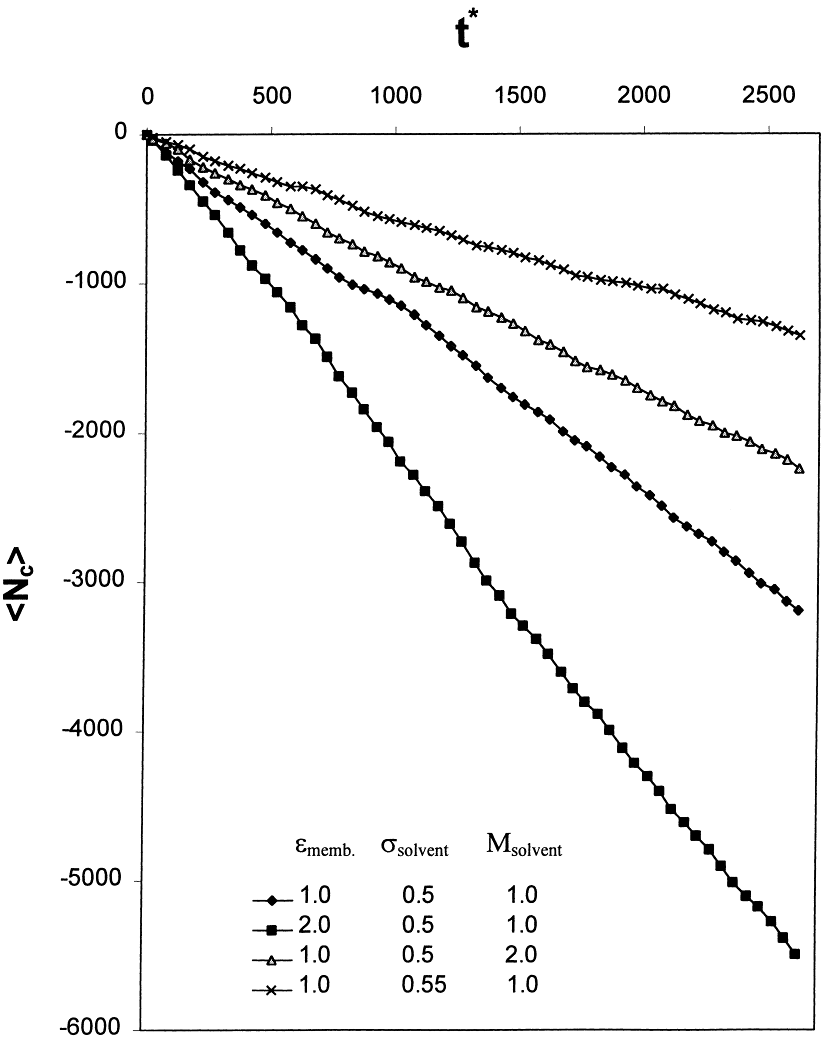

Fig. 7. Effect of changing $\varepsilon_{\text{membrane}}$, σ_{solvent}, and M_{solvent} on the solvent permeation rate across the semi-permeable membrane at a higher temperature, T^*=1.25, compared to 1.075 shown earlier.

molecules near the membrane. The osmotic driving force in the system, which in this case is mostly due to the difference in density (and consequently the pressure) between the solution and solvent compartment, can then force these solvent molecules across the membrane. It is also evident that the increased attraction between the solvent molecule and the membrane does not significantly reduce the diffusion of the molecules across the membrane, as can be seen from Fig. 5. This result could have important industrial implications. It shows that a membrane, which has stronger interactions with the solvent molecules, can increase the permeability of the membrane, in addition to affecting the selectivity of the membrane [16].

The effect of changing M_{solvent} is also shown in Figs. 3–5. In this case as expected the density profiles are not significantly affected. The decrease in solvent permeation rate is primarily due to the decreased mobility of the solvent molecules resulting from the increased molecular mass, as can be seen from Fig. 5. It also appears that the decrease in the solvent diffusion rate roughly follows the rule that diffusion coefficients vary inversely with $M^{1/2}$.

Finally the effect of increasing σ_{solvent} from 0.5 to 0.55 is also included in Figs. 3–5. As expected this results in a considerable lowering of the solvent permeation rate, as the pore to solvent diameter ratio is now smaller. This lowering is caused by a decrease in the solvent diffusion rate, which can be seen clearly in Fig. 5. The density profiles are relatively unaffected by the change in solvent diameter, as shown in Fig. 4 and must not play any significant direct role in lowering the permeation rate.

We have also examined the effect of intermolecular forces on the permeation rates at a higher solute concentration of $N_{\text{B}}=40$. This decreases the osmotic driving force somewhat, as the higher concentration increases the osmotic pressure of the solution. These results are shown in Fig. 6. In this case the effect of increasing $\varepsilon_{\text{membrane}}$ to 2.0 from 1.0 is more significant, and increases the permeation rate almost by a factor of 3. It also appears that it takes longer for the system to reach its "final" steady state permeation rate (at $t^*\approx 500$). With a lower driving force across the membrane, the presence of additional solvent molecules due to the increased interaction between the solvent molecules and the membrane seems to have an even greater effect on the permeation rate. The effect of the change in M_{solvent} to 2.0 from 1.0 appears to lower the permeation rate about 20%, somewhat less than the 30% drop found at the lower concentration. The decrease in the diffusion coefficient of the solvent molecules due to the change in the molecular weight in the two cases is however similar. These results point to the less important role of the diffusion rate of the solvent when the driving force is weaker, as do the results when σ_{solvent} is increased from 0.5 to 0.55. They show a drop of 70% compared to the 75% drop found at the lower concentration.

The effect of changes in intermolecular forces in the system were also studied at a higher temperature, $T^*=1.25$ with $\rho^*=1.0$, and a lower density, $\rho^*=0.746$ with $T^*=1.075$. The results were found to be in qualitative agreement with the results shown in Figs. 3–5 (for $T^*=1.075$ and $\rho^*=1.0$), as evidenced by the results for the higher temperature case shown in Fig. 7. Changes in solvent permeation rates due to changes in density and temperature, while keeping all the other parameters constant, are shown in Fig. 8. It appears that the solvent permeation rate is rather sensitive to the temperature of the system, but is less sensitive to the density of the system. This we believe is primarily due to the increased diffusion rate of the solvents at higher temperature. At lower densities the solvent diffusion rate is higher, but there are fewer solvent molecules near the membrane, and thus the solvent mass transport rate is relatively unaffected.

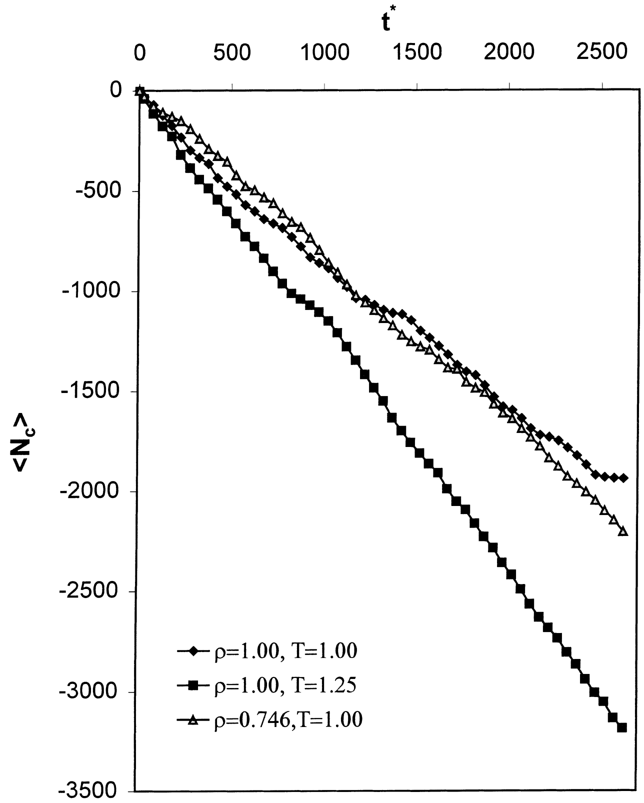

Fig. 8. Effect of changes in system density and temperature on the solvent permeation rate across the semi-permeable membrane, when the intermolecular force potential parameters are otherwise equal.

Finally, we have also looked at the effect of the thickness of the membrane on the solvent permeation rate. We have compared the permeation rates for type I and type II membranes for comparable systems at state conditions similar to those shown in Figs. 3–5. Because of the finite size of the system it is not possible to study densities and concentrations that are exactly equal, but these small differences were practically insignificant. Results are shown in Fig. 9. These studies were carried out with a time step $\Delta t^*(\Delta t\sqrt{\varepsilon/M}/\sigma) = 0.0020$ and solvent recycling every 5000 steps. As expected going from membrane type I to II lowered the solvent permeation rate. This decrease was

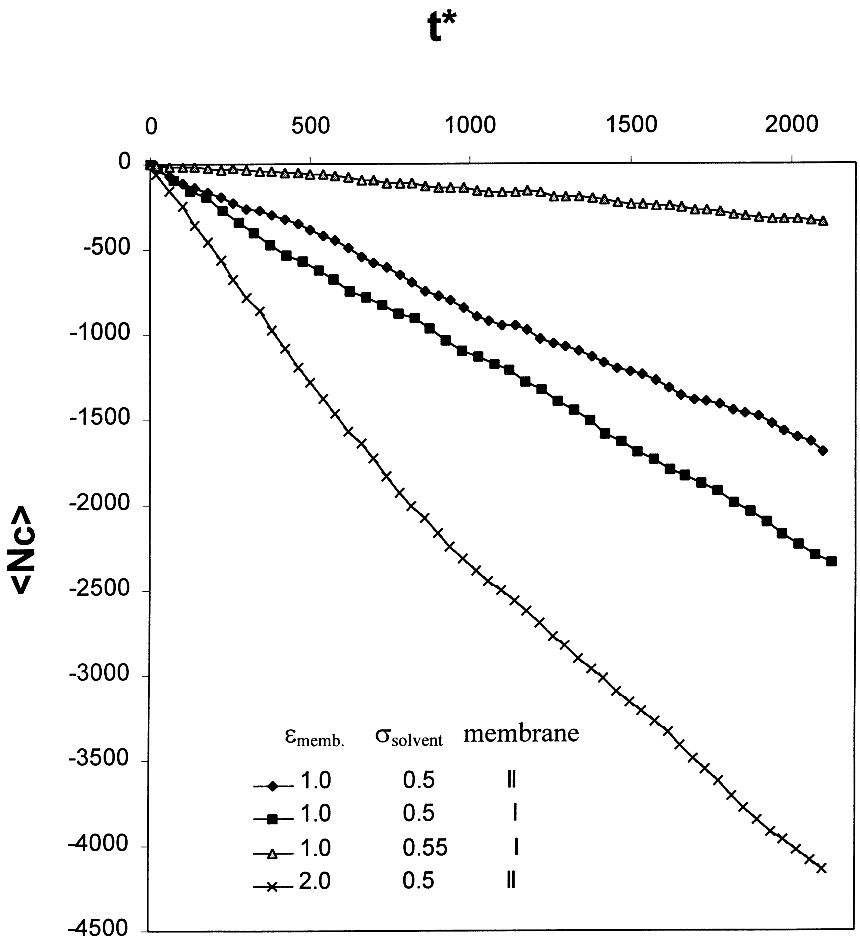

Fig. 9. Effect of membrane morphology on the solvent permeation rate across the semi-permeable membrane. Type I membrane has only one layer of molecules, while type II membrane has two such layers (see Section 2 for more details).

found to be about 25%. As stated earlier, the type II membrane has almost double the thickness of the type I membrane. We also examined the effect of changing the $\varepsilon_{\mathrm{membrane}}$ for type II membranes, and this is also shown in Fig. 9. The effect of increasing $\varepsilon_{\mathrm{membrane}}$ from 1.0 to 2.0 is to increase the permeation rate by about a factor of 2.5, compared to a factor of 2.0 for type I membrane. This shows that for thicker membranes increased interaction between the solvent and the membrane is even more important than for thinner membranes. When we increased $\sigma_{\mathrm{solvent}}$ for type II membranes from 0.5 to 0.55 this resulted in lowering the permeation rate by about 85%. This is somewhat larger than the 75% decrease found in type I membranes, pointing to the expected stronger influence of the pore to solvent diameter ratio in the case of thicker membranes.

4. Conclusions

A new molecular dynamics simulation method to study osmosis and reverse osmosis at steady state has been developed and used to study the effect of intermolecular forces, state conditions, and membrane thickness on the solvent permeation rate across the membrane. Our results show that membranes that have stronger interactions with the solvent molecules have significantly larger solvent permeation rates, especially when the osmotic driving forces are weaker. In addition the permeation rates increase significantly with increases in temperature, but the density does not appear to affect the permeation rate as much. Finally, as could have been expected, the thickness of the membrane also has a large effect on the solvent permeation rate. These results could be used to test both micro-continuum hydrodynamic theories [4] as well as other statistical mechanical theories for semi-permeable membranes [19].

Acknowledgements

This research was supported by a grant from the Division of Chemical Sciences, US Department of Energy (No. DE-FGO2-96ER14680).

References

[1] M.P. Allen, D.J. Tildesley, Computer Simulation of Liquids, Clarendon Press, Oxford, 1987.

[2] S. Murad, P. Ravi, J.G. Powles, J. Chem. Phys. 98 (1993) 9971.

[3] C.R.A. Catlow, Phys. World (1997) 28.

[4] T. Chou, Phys. Rev. Lett. 80 (1998) 85.

[5] D.C. Guell, H. Brenner, Ind. Eng. Chem. Res. 35 (1996) 3004.

[6] W.M. Deen, AIChE J. 33 (1987) 1409.

[7] S. Murad, J.G. Powles, J. Chem. Phys. 99 (1993) 7271.

[8] S. Murad, Adsorption 2 (1996) 95.

[9] F. Paritosh, S. Murad, AIChE J. 42 (1996) 2984.

[10] S. Murad, R. Madhusudan, J.G. Powles, Mol. Phys. 90 (1997) 671.

[11] D. Hirshfeld, Y. Radzyner, D.C. Rapaport, Phys. Rev. E 56 (1997) 4404.

[12] J.M.D. MacElroy, J. Chem. Phys. 101 (1994) 5274.

[13] G.S. Heffelfinger, F. Van Swol, J. Chem. Phys. 100 (1994) 7548.

[14] N. Metropolis, A.W. Rosenbluth, M.N. Rosenbluth, A.H. Teller, E. Teller, J. Chem. Phys. 21 (1953) 1087.

[15] A.Z. Panagiotopoulos, N. Quirke, M. Stapleton, D.J. Tildesley, Mol. Phys. 63 (1988) 527.

[16] B.S. Parekh, Reverse Osmosis Technology, Marcel Dekker, New York, 1988.

[17] J.M. Haile, Molecular Dynamics, Elementary Methods, Wiley, New York, 1992.

[18] R.T. Yang, Gas Separation by Adsorption Processes, Butterworth, New York, 1987.

[19] P. Bryk, A. Patrykiejew, O. Pazio, S. Sokolowski, Mol. Phys. 93 (1998) 111.